

**Repository of the Max Delbrück Center for Molecular Medicine (MDC)
in the Helmholtz Association**

<https://edoc.mdc-berlin.de/17087/>

**A gain-of-function mutation in the CLCN2 chloride channel gene causes
primary aldosteronism**

Fernandes-Rosa F.L., Daniil G., Orozco I.J., Göppner C., El Zein R., Jain V., Boulkroun S.,
Jeunemaitre X., Amar L., Lefebvre H., Schwarzmayr T., Strom T.M., Jentsch T.J., Zennaro M.C.

This is the final version of the accepted manuscript. The original article has been published in final edited form in:

Nature Genetics
2018 MAR; 50(3), 355–361
2018 FEB 05 (first published online: final publication)
Doi: [10.1038/s41588-018-0053-8](https://doi.org/10.1038/s41588-018-0053-8)

URL: <https://www.nature.com/articles/s41588-018-0053-8>

Publisher: [Nature America](#) (Springer Nature)
Copyright © 2018 Nature America Inc., part of Springer Nature. All rights reserved.

Publisher's notice

This is a post-peer-review, pre-copyedit version of an article published in *Nature Genetics*. The final authenticated version is available online at: <https://dx.doi.org/10.1038/s41588-018-0053-8>.

A gain-of-function mutation in the *CLCN2* chloride channel gene causes primary aldosteronism

Fabio L. Fernandes-Rosa^{1,2,3*#}, Georgios Daniil^{1,2*}, Ian J. Orozco^{4,5*}, Corinna Göppner^{4,5§}, Rami El Zein^{1,2§}, Vandana Jain^{6^}, Sheerazed Boulkroun^{1,2^}, Xavier Jeunemaitre^{1,2,3}, Laurence Amar^{1,2,7}, Hervé Lefebvre^{8,9,10}, Thomas Schwarzmayr¹¹, Tim M. Strom^{11,12}, Thomas J. Jentsch^{4,5#}, Maria-Christina Zennaro^{1,2,3#}

¹INSERM, UMRS_970, Paris Cardiovascular Research Center, Paris, France

²Université Paris Descartes, Sorbonne Paris Cité, Paris, France

³Assistance Publique-Hôpitaux de Paris, Hôpital Européen Georges Pompidou, Service de Génétique, Paris, France

⁴Leibniz-Forschungsinstitut für Molekulare Pharmakologie (FMP), Berlin, Germany

⁵Max-Delbrück-Centrum für Molekulare Medizin (MDC), Berlin, Germany

⁶Division of Pediatric Endocrinology, Department of Pediatrics, All India Institute of Medical Sciences, New Delhi, India

⁷Assistance Publique-Hôpitaux de Paris, Hôpital Européen Georges Pompidou, Unité Hypertension artérielle, Paris, France

⁸Normandie Univ, UNIROUEN, Rouen, France

⁹INSERM, DC2N, Rouen, France

¹⁰Department of Endocrinology, Diabetes and Metabolic Diseases, University Hospital of Rouen, Rouen, France

¹¹Institute of Human Genetics, Helmholtz Zentrum München, Neuherberg, Germany

¹²Institute of Human Genetics, Technische Universität München, Munich, Germany

*,[§],[^] equal contribution

#Corresponding authors

Address correspondence to:

Maria-Christina Zennaro, MD, PhD

INSERM, U970

Paris Cardiovascular Research Center – PARCC

56, rue Leblanc,

75015 Paris – France

Tel : +33 (0)1 53 98 80 42

Fax : + 33 (0)1 53 98 79 52

e-mail : maria-christina.zennaro@inserm.fr

Fabio Fernandes Rosa, MD, PhD

INSERM, U970

Paris Cardiovascular Research Center – PARCC

56, rue Leblanc,

75015 Paris – France

Tel : +33 (0)1 53 98 80 43

Fax : + 33 (0)1 53 98 79 52

e-mail : fabio.fernandes-rosa@inserm.fr

Thomas J. Jentsch, MD, PhD

FMP / MDC

Robert-Rössle-Strasse 10

13125 Berlin – Germany

Tel: +49 30 9406 2961
Fax: +49 30 9406 2960
e-mail: Jentsch@fmp-berlin.de

INTRODUCTORY PARAGRAPH

Primary aldosteronism is the most common and curable form of secondary arterial hypertension. We performed whole exome sequencing in patients with early-onset primary aldosteronism and identified a *de novo* heterozygous c.71G>A/p.Gly24Asp mutation in the *CLCN2* gene, coding for the voltage-gated ClC-2 chloride channel¹, in a patient diagnosed at age 9 ys. Patch-clamp analysis of glomerulosa cells of mouse adrenal gland slices revealed hyperpolarization-activated Cl⁻ currents that were abolished in *Clcn2*^{-/-} mice. The p.Gly24Asp mutation, located in a well conserved ‘inactivation domain’^{2,3}, abolished the voltage- and time-dependent gating of ClC-2 and strongly increased Cl⁻ conductance at resting potentials. Expression of ClC-2_{24Asp} in adrenocortical cells increased expression of aldosterone synthase and aldosterone production.

Our data indicate that *CLCN2* mutations cause primary aldosteronism. They highlight for the first time the important role of chloride in aldosterone biosynthesis and identify ClC-2 as the foremost chloride conductor of resting glomerulosa cells.

1 **MAIN TEXT**

2 Arterial hypertension is a major cardiovascular risk factor ⁴. Primary aldosteronism is
3 the most common and curable form of secondary arterial hypertension, with an estimated
4 prevalence of ~10% in referred patients and 4% in primary care⁵, and up to 20% of patients
5 with resistant hypertension ⁶. Primary aldosteronism results from autonomous aldosterone
6 production in the adrenal cortex ⁷, caused in most cases by a unilateral aldosterone-producing
7 adenoma or bilateral adrenal hyperplasia (BAH). It is diagnosed on the basis of hypertension
8 associated with increased aldosterone to renin ratio and often hypokalemia ⁸. Compared to
9 essential hypertension, increased aldosterone levels in primary aldosteronism are associated
10 with increased cardiovascular risk in particular coronary artery disease, heart failure, renal
11 damage and stroke ^{9,10}.

12 Gain-of-function mutations in different genes, coding for cation channels (*KCNJ5* ¹¹,
13 *CACNAID* ^{12,13}, *CACNAIH* ^{14,15}) and ATPases (*ATP1A1* and *ATP2B3*, ^{12,16}), regulating
14 intracellular ion homeostasis and plasma membrane potential, have been described in
15 aldosterone producing adenoma and familial forms of primary aldosteronism, but the
16 pathophysiology of many cases is still unknown.

17 We performed whole exome sequencing on germline DNA from 12 patients with young onset
18 hypertension and hyperaldosteronism diagnosed before age 25 ys. Two index cases were
19 investigated together with their parents and unaffected sibling to search for *de novo* variants.
20 A *de novo* germline *CLCN2* variant c.71G>A (NM_004366; p.Gly24Asp) was identified in
21 subject K1011-1, but not in her asymptomatic parents (K1011-3 and K1011-4) and sibling
22 (K1011-2, Fig. 1a and 1b, Table 1). The variant was absent from more than 120.000 alleles in
23 the Exome Aggregation Consortium (ExAC) and in our in-house database. We did not find
24 additional *CLCN2* variants among the other 11 investigated individuals. *CLCN2* encodes the
25 chloride channel ClC-2. The variant *CLCN2* p.Gly24Asp localizes to its N-terminal
26 cytoplasmic domain (Fig. 1c, d). Gly24 is highly conserved in ClC-2 orthologs of species as
27 distant as zebrafish and *Xenopus* (Fig. 1c).

28 The patient carrying the *CLCN2* p.Gly24Asp variant is a 9 year old girl, who presented
29 with severe headache and vomiting lasting for 1 year (Table 1). The child was
30 developmentally normal, first born to a non-consanguineous couple. There was history of
31 mild hypertension in maternal grandmother and granduncle. Blood pressure (BP) was 172/100
32 mm Hg, heart rate was 120/minute. The rest of the examination was normal. Her work-up
33 revealed persistent hypokalemia (serum K⁺ ranging from 1.8 to 2.4 meq/L), elevated serum
34 aldosterone (868.1 pg/ml, reference range 12-340 pg/ml) and suppressed plasma renin activity
35 (0.11 ng/ml/hr, reference range 1.9 to 6.0 ng/ml/hr in upright posture), suggestive of primary
36 aldosteronism. Abdominal CT scan showed no adrenal abnormalities. Other parameters
37 including 24 hours urinary vanillylmandelic acid and serum cortisol were normal.
38 Hypertension was initially managed with amlodipin, enalapril and atenolol. Once the
39 diagnosis of primary aldosteronism was made, spironolactone was added, enalapril was
40 stopped and doses of amlodipin and atenolol were reduced. Serum K⁺ normalized. A positive
41 glucocorticoid suppression test (aldosterone 949.3 pg/ml at baseline and 56.9 pg/ml after

42 administration of oral dexamethasone 0.5 mg every 6 hours for 48 hours) suggested the
43 possibility of glucocorticoid remediable aldosteronism (GRA), a rare familial form of
44 hyperaldosteronism¹⁷. However, genetic analysis for a chimeric *CYP11B1/CYP11B2* gene
45 was negative. The child's hypertension has been well controlled over the last 18 months with
46 prednisolone 5mg/m²/day, spironolactone and amlodipin. On treatment, her serum aldosterone
47 and plasma renin are 421 pg/ml (reference range 25 to 392) and 8.22 μU/mL (4.4 to 46.1).
48 After exclusion of GRA by genetic testing, prednisolone treatment was stopped.

49 Cl⁻ conductances can regulate the excitability of neuronal, muscle, and endocrine cells
50¹⁸⁻²¹. In zona glomerulosa cells, ACTH-activated Cl⁻ currents have been described²², but their
51 outward rectification sets them apart from hyperpolarization-activated ClC-2 currents. ClC-2
52 is expressed in almost all tissues¹ and may have roles in ion homeostasis and transepithelial
53 transport²³. *Clcn2*^{-/-} mice display early postnatal retinal and testicular degeneration²⁴ as well
54 as leukodystrophy^{25,26}; in humans, *CLCN2* loss-of-function mutations result in
55 leukodystrophy²⁷ that may be associated with azoospermia²⁸. These phenotypes have been
56 ascribed to a role of ClC-2 in extracellular ion homeostasis^{24,25}.

57 Data retrieved from a transcriptome analysis including eleven human adrenals²⁹
58 showed high expression of *CLCN2* in human adrenal cortex (Supplementary Table 1). In
59 mice, Western blots revealed similar expression of ClC-2 in whole adrenal gland as in brain
60 (Fig. 2a), which expresses substantial, physiologically important amounts of ClC-2²⁵. Patch-
61 clamp analysis of glomerulosa cells *in situ* revealed typical hyperpolarization-activated
62 currents in WT, but not in *Clcn2*^{-/-} mice (Fig. 2 b,c). Their magnitude was similar to those
63 observed in Bergmann glia which prominently express ClC-2²⁶. The almost complete
64 absence of Cl⁻ currents in *Clcn2*^{-/-} cells demonstrates that under resting conditions ClC-2
65 mediates the bulk of glomerulosa cell Cl⁻ currents.

66 The *CLCN2* p.Gly24Asp mutation is located in a highly conserved ‘inactivation
67 domain’^{2,3} of the channel. Deletions and point mutations in this region and an intracellular
68 loop² (highlighted in Fig. 1c, d) lead to ‘open’ CIC-2 channels that have lost their sensitivity
69 to voltage, cell swelling, or external pH^{2,3}. Likewise, insertion of the p.Gly24Asp mutation
70 drastically changed voltage-dependent gating of CIC-2 (Fig. 2d,e,h) and dramatically
71 increased current amplitudes when expressed in *Xenopus* oocytes (Fig. 2d-g). When measured
72 at -80 mV, the approximate resting potential of glomerulosa cells³⁰, current amplitudes from
73 the mutant channel were much larger compared to WT (Fig. 2d-f). Linear, ohmic currents like
74 those of the mutant channel might be due to unspecific electrical leaks; however, currents of
75 both WT and mutant CIC-2 were markedly reduced when extracellular chloride was replaced
76 by iodide (Fig. 2d-f), agreeing with the Cl⁻>I⁻ selectivity of CLC channels in general²³ and
77 CIC-2 in particular¹. The activation of CIC-2 by acid extracellular pH can be almost
78 abolished by mutations in the ‘inactivation domain’². Likewise, the CIC-2_{24Asp} mutant had
79 largely reduced pH sensitivity (Fig. 2i-j, Supplementary Fig.1). In conclusion, the
80 p.Gly24Asp mutation results in a strong gain of function, explaining the dominant disease
81 phenotype of the mutation that is present at the heterozygote state. It also suggests a
82 pathophysiological mechanism in which a strong increase in Cl⁻ currents may depolarize
83 glomerulosa cells, thereby opening voltage-gated Ca²⁺ channels and activating transcriptional
84 programs via an increase of cytosolic Ca²⁺.

85 Expression of the mutant CIC-2_{24Asp} channel in adrenocortical H295R-S2 cells, and
86 conversely, knock-down of CIC-2 by shRNA significantly affected aldosterone production
87 and expression of steroidogenic enzymes. Despite similar expression of CIC-2 in H295R-S2
88 cells stably transfected with CIC-2_{24Asp} or CIC-2_{WT} (Fig. 3a and 3b), aldosterone synthase
89 expression (Fig. 3a and 3c) and aldosterone production (Fig. 3d, e) were significantly
90 increased in CIC-2_{24Asp} expressing cells. Stimulation with angiotensin II (AngII 10nM) or K⁺

91 (12mM) increased aldosterone production in cells expressing WT CIC-2 (Fig. 3e). A further
92 increase was observed in cells expressing CIC-2_{24Asp} after AngII stimulation, but not after K⁺
93 stimulation (Fig. 3e). Nevertheless, also after stimulation, aldosterone production in cells
94 expressing CIC-2_{24Asp} was significantly higher compared to cells expressing CIC-2_{WT} (Fig.
95 3e). Infection of H295R-S2 cells with CIC-2 shRNA reduced *CLCN2* expression by ~50%
96 (Supplementary Fig. 2a) compared with a scrambled shRNA, and significantly reduced
97 aldosterone production, both at baseline and after stimulation (Supplementary Fig. 2b),
98 suggesting that even WT CIC-2 currents, although much smaller than currents from the
99 Gly24Asp mutant, significantly increase the excitability of H295R-S2 adrenocortical cells.
100 These changes were paralleled in both models by concomitant modifications of the expression
101 of steroidogenic genes. A significant increase of mRNA expression of *CYP11B2* (encoding
102 aldosterone synthase, Fig. 3f), *StAR* (encoding the Steroidogenic acute regulatory protein, Fig.
103 3g) and *CYP21A2* (encoding Steroid 21-hydroxylase, Fig. 3h) was observed in CIC-2_{24Asp}
104 compared with CIC-2_{WT} overexpressing cells in basal conditions. AngII increased expression
105 of *StAR* and *CYP11B2*, while K⁺ stimulation increased mRNA expression of *CYP11B2*.
106 Conversely, knock-down of CIC-2 led to a significant decrease in *CYP11B2* expression in all
107 conditions (Supplementary Fig. 2c). These data further support the notion that a gain-of-
108 function *CLCN2* mutation may depolarize the cell, activate the steroidogenic pathway, and
109 increase aldosterone production. While knock-down of CIC-2 influences aldosterone
110 production in H295R-S2 cells which have a resting potential of about – 65 mV (Fig. 4a, b),
111 this may not be the case in native glomerulosa cells. Because their V_m is close to the K⁺
112 equilibrium potential³⁰, they are unlikely to markedly hyperpolarize upon loss of CIC-2. No
113 changes of blood pressure have been reported for mice or patients lacking CIC-2^{24,25,27}, but
114 this issue has not been investigated in detail.

115 We next explored the effect of the ClC-2 Gly24Asp mutation on the membrane
116 potential and on calcium influx through voltage-gated calcium channels. These studies were
117 performed with the perforated patch clamp technique which does not disturb the intracellular
118 chloride concentration and is required to see the full effect of 'inactivation domain'^{2,3}
119 mutations^{31,32}. In the stably transfected H295R-S2 cells used to investigate steroidogenesis
120 (Fig. 3), there was a trend of V_m to be depolarized in ClC-2_{24Asp} transfected compared to ClC-
121 2_{WT} transfected cells (mean values of roughly -52 and -67 mV, respectively) (Fig. 4a).
122 However, because these cell lines are not clonal, the variability was large and the difference
123 was not statistically significant.

124 We therefore resorted to transient transfection of H295R-S2 cells which allowed us to
125 select ClC-2 expressing cells by fluorescence of co-transfected GFP (Fig. 4b-g). Although
126 these cells express ClC-2 less efficiently than *Xenopus* oocytes (compare Fig. 4f and 2d) and
127 HEK cells^{31,32}, ClC-2_{24Asp} expressing cells displayed robust chloride currents that lacked
128 strong voltage-dependence (Fig. 4c-g). The observed increase in currents may reflect both an
129 increase in currents per channel and in the number of channels; both must be considered when
130 analyzing pathogenic effects of ion channel mutants. This increase in currents correlated with a
131 strong depolarization from $V_m = -65 \pm 4$ (ClC-2_{WT}) to -46 ± 4 mV in ClC-2_{24Asp} transfected
132 cells (Fig. 4b), indicating that chloride concentration in H295R-S2 cells is higher than
133 predicted by the electrochemical equilibrium. This depolarization may open voltage-
134 dependent calcium channels. Indeed, nifedipine (an L-type calcium channel blocker) and/or
135 mibefradil (a T-type calcium channel blocker) strongly reduced aldosterone production in
136 cells expressing the ClC-2_{24Asp} mutant (Fig. 4i). The involvement of L-type calcium channels
137 appeared to be larger in ClC-2_{24Asp} expressing cells (Fig. 4h), possibly because of their
138 depolarized plasma membrane potential which is required to open these channels³³. However,

139 we cannot exclude that nifedipine acted partially through T-type calcium channels, which are
140 also blocked by this compound at depolarized voltages³⁴.

141 To investigate whether the *CLCN2* p.Gly24Asp mutation could be involved in other
142 forms of primary aldosteronism, we sequenced exon 2 of *CLCN2* in 100 patients with BAH.
143 While *CLCN2* p.Gly24Asp was not identified among these subjects, we identified two rare
144 *CLCN2* variants, c.197G>A (p.Arg66Gln, rs755883734) and c.143C>G (p.Pro48Arg,
145 rs115661422) in two subjects (Supplementary Fig. 3). Minor allele frequencies of these
146 variants are very low in the ExAC database (*CLCN2* p.Arg66Gln 0.00003; *CLCN2*
147 p.Pro48Arg 0.0017). Both variants failed to significantly change CIC-2 currents in
148 heterologous expression (Supplementary Fig. 4), in spite of a previously described³⁵ moderate
149 reduction of CIC-2_{Pro48Arg} current amplitudes. Nonetheless, it is noteworthy that the two
150 patients were diagnosed with hypertension at young age, 29 and 19 ys respectively (Table 1)
151 and in both cases during pregnancy. Finally, sequencing the *CLCN2* exons encoding the N-
152 terminal domain (exon 1 and 2) and the loop between helices J and K (exon 10),
153 corresponding to the CIC-2 ‘inactivation domains’^{2,3}, in 20 additional patients with
154 hypertension before age 20 did not identify additional mutations. Among these patients, nine
155 had a history of hypertension before the age of 15 years (one before age 10 ys), indicating that
156 *CLCN2* mutations might underlie very young onset forms of primary aldosteronism.

157 In conclusion, we show that a gain-of-function mutation in the CIC-2 chloride channel
158 underlies a genetic form of secondary arterial hypertension and identify CIC-2 as the foremost
159 chloride conductor of resting glomerulosa cells. We suggest that increased Cl⁻ currents
160 induced by the CIC-2 p.Gly24Asp mutation could depolarize the zona glomerulosa cell
161 membrane, thereby opening voltage-gated calcium channels which trigger autonomous
162 aldosterone production by increasing intracellular Ca²⁺ concentrations (Fig. 5b, red arrows).
163 We hypothesize that the increased Cl⁻ currents may overcome the hyperpolarizing currents of

164 K^+ channels that normally determine the glomerulosa cell resting potential. The inhibition of
165 these potassium channels e.g. upon AngII stimulation, or the depolarizing currents mediated
166 by these channels upon increases in extracellular K^+ , are the main mechanisms triggering
167 aldosterone production under physiological conditions (Fig. 5a, dashed black arrows).

168 Not only mutations in the amino-terminal CIC-2 'inactivation domain'^{2,3}, like the
169 Gly24Asp mutation found here, but also in the cytoplasmic linker between transmembrane
170 helices J and K may cause primary aldosteronism (Fig. 1d). Several point mutations in that
171 linker result in constitutively open CIC-2 channels². We propose both regions as potential
172 hotspots for mutations causing primary aldosteronism. The discovery that a chloride channel
173 is involved in primary aldosteronism opens new and unexpected perspectives for the
174 pathogenesis and treatment of arterial hypertension.

175

176 **Acknowledgements**

177 This work was funded through institutional support from INSERM and by the Agence
178 Nationale pour la Recherche (ANR-13-ISV1-0006-01), the Fondation pour la Recherche
179 Médicale (DEQ20140329556), the Programme Hospitalier de Recherche Clinique (PHRC
180 grant AOM 06179), and by institutional grants from INSERM. The laboratory of Dr. Maria-
181 Christina Zennaro is also partner of the H2020 project ENSAT-HT grant n° 633983. Thomas
182 J. Jentsch was supported by institutional funding from the Leibniz and Helmholtz
183 Associations, a grant from the BMBF (E-RARE 01GM1403) and by the Prix Louis-Jeantet de
184 Médecine.

185

186 **Conflict of interest**

187 The authors have nothing to disclose.

188

189 **Author Contributions**

190 MCZ, FFR, GD, IJO and TJJ designed experiments and wrote the manuscript. TMS, MCZ,
191 TS and FFR performed and analyzed whole exome sequencing. MCZ, FFR, GD, REZ and
192 SB performed and analyzed *in vitro* studies on H295R-S2 cells. IJO performed
193 electrophysiological studies that were analyzed by IJO and TJJ. CG characterized adrenal
194 glands from WT and *Cln2*^{-/-} mice and performed Western blots. VJ, XJ, LA, and HL were
195 responsible for patients' recruitment, medical care and clinical data acquisition. All authors
196 revised the manuscript draft.

197

198

199

200 **References**

- 201 1. Thiemann, A., Grunder, S., Pusch, M. & Jentsch, T.J. A chloride channel widely
202 expressed in epithelial and non-epithelial cells. *Nature* **356**, 57-60 (1992).
- 203 2. Jordt, S.E. & Jentsch, T.J. Molecular dissection of gating in the CIC-2 chloride
204 channel. *EMBO J.* **16**, 1582-92 (1997).
- 205 3. Grunder, S., Thiemann, A., Pusch, M. & Jentsch, T.J. Regions involved in the opening
206 of CIC-2 chloride channel by voltage and cell volume. *Nature* **360**, 759-62 (1992).
- 207 4. Worldwide trends in blood pressure from 1975 to 2015: a pooled analysis of 1479
208 population-based measurement studies with 19.1 million participants. *Lancet* **389**, 37-
209 55 (2017).
- 210 5. Hannemann, A. & Wallaschofski, H. Prevalence of primary aldosteronism in patient's
211 cohorts and in population-based studies--a review of the current literature. *Horm.*
212 *Metab. Res.* **44**, 157-62 (2012).
- 213 6. Calhoun, D.A. Hyperaldosteronism as a common cause of resistant hypertension.
214 *Annu. Rev. Med.* **64**, 233-47 (2013).
- 215 7. Zennaro, M.C., Boulkroun, S. & Fernandes-Rosa, F. Genetic Causes of Functional
216 Adrenocortical Adenomas. *Endocr. Rev.* **38**, 516-537 (2017).
- 217 8. Funder, J.W. *et al.* The Management of Primary Aldosteronism: Case Detection,
218 Diagnosis, and Treatment: An Endocrine Society Clinical Practice Guideline. *J. Clin.*
219 *Endocrinol. Metab.* **101**, 1889-916 (2016).
- 220 9. Savard, S., Amar, L., Plouin, P.F. & Steichen, O. Cardiovascular complications
221 associated with primary aldosteronism: a controlled cross-sectional study.
222 *Hypertension* **62**, 331-6 (2013).
- 223 10. Rossi, G.P. *et al.* A prospective study of the prevalence of primary aldosteronism in
224 1,125 hypertensive patients. *J. Am. Coll. Cardiol.* **48**, 2293-300 (2006).

- 225 11. Choi, M. *et al.* K⁺ channel mutations in adrenal aldosterone-producing adenomas and
226 hereditary hypertension. *Science* **331**, 768-72 (2011).
- 227 12. Azizan, E.A. *et al.* Somatic mutations in ATP1A1 and CACNA1D underlie a common
228 subtype of adrenal hypertension. *Nat. Genet.* **45**, 1055-60 (2013).
- 229 13. Scholl, U.I. *et al.* Somatic and germline CACNA1D calcium channel mutations in
230 aldosterone-producing adenomas and primary aldosteronism. *Nat. Genet.* **45**, 1050-4
231 (2013).
- 232 14. Scholl, U.I. *et al.* Recurrent gain of function mutation in calcium channel CACNA1H
233 causes early-onset hypertension with primary aldosteronism. *Elife* **4**, e06315 (2015).
- 234 15. Daniil, G. *et al.* CACNA1H Mutations Are Associated With Different Forms of
235 Primary Aldosteronism. *EBioMedicine* **13**, 225-236 (2016).
- 236 16. Beuschlein, F. *et al.* Somatic mutations in ATP1A1 and ATP2B3 lead to aldosterone-
237 producing adenomas and secondary hypertension. *Nat. Genet.* **45**, 440-4, 444e1-2
238 (2013).
- 239 17. Lifton, R.P. *et al.* A chimaeric 11beta-hydroxylase aldosterone synthase gene causes
240 glucocorticoid-remediable aldosteronism and human hypertension. *Nature* **355**, 262-
241 265 (1992).
- 242 18. Moss, S.J. & Smart, T.G. Constructing inhibitory synapses. *Nat. Rev. Neurosci.* **2**,
243 240-50 (2001).
- 244 19. Rinke, I., Artmann, J. & Stein, V. ClC-2 voltage-gated channels constitute part of the
245 background conductance and assist chloride extrusion. *J. Neurosci.* **30**, 4776-86
246 (2010).
- 247 20. Koch, M.C. *et al.* The skeletal muscle chloride channel in dominant and recessive
248 human myotonia. *Science* **257**, 797-800 (1992).

- 249 21. Guo, J.H. *et al.* Glucose-induced electrical activities and insulin secretion in
250 pancreatic islet beta-cells are modulated by CFTR. *Nat. Commun.* **5**, 4420 (2014).
- 251 22. Chorvatova, A., Gendron, L., Bilodeau, L., Gallo-Payet, N. & Payet, M.D. A Ras-
252 dependent chloride current activated by adrenocorticotropin in rat adrenal zona
253 glomerulosa cells. *Endocrinology* **141**, 684-92 (2000).
- 254 23. Jentsch, T.J. Discovery of CLC transport proteins: cloning, structure, function and
255 pathophysiology. *J. Physiol.* **593**, 4091-109 (2015).
- 256 24. Bosl, M.R. *et al.* Male germ cells and photoreceptors, both dependent on close cell-
257 cell interactions, degenerate upon CLC-2 Cl⁻ channel disruption. *EMBO J.* **20**, 1289-
258 99 (2001).
- 259 25. Blanz, J. *et al.* Leukoencephalopathy upon disruption of the chloride channel CLC-2. *J.*
260 *Neurosci.* **27**, 6581-9 (2007).
- 261 26. Hoegg-Beiler, M.B. *et al.* Disrupting MLC1 and GlialCAM and CLC-2 interactions in
262 leukodystrophy entails glial chloride channel dysfunction. *Nat. Commun.* **5**, 3475
263 (2014).
- 264 27. Depienne, C. *et al.* Brain white matter oedema due to CLC-2 chloride channel
265 deficiency: an observational analytical study. *Lancet Neurol.* **12**, 659-68 (2013).
- 266 28. Di Bella, D. *et al.* Subclinical leukodystrophy and infertility in a man with a novel
267 homozygous CLCN2 mutation. *Neurology* **83**, 1217-8 (2014).
- 268 29. Boulkroun, S. *et al.* Prevalence, Clinical, and Molecular Correlates of KCNJ5
269 Mutations in Primary Aldosteronism. *Hypertension* **59**, 592-8 (2012).
- 270 30. Spat, A. & Hunyady, L. Control of aldosterone secretion: a model for convergence in
271 cellular signaling pathways. *Physiol. Rev.* **84**, 489-539 (2004).

- 272 31. Varela, D., Niemeyer, M.I., Cid, L.P. & Sepulveda, F.V. Effect of an N-terminus
273 deletion on voltage-dependent gating of the ClC-2 chloride channel. *J. Physiol.* **544**,
274 363-72 (2002).
- 275 32. Pusch, M., Jordt, S.E., Stein, V. & Jentsch, T.J. Chloride dependence of
276 hyperpolarization-activated chloride channel gates. *J. Physiol.* **515 (Pt 2)**, 341-53
277 (1999).
- 278 33. Barrett, P.Q. *et al.* Role of voltage-gated calcium channels in the regulation of
279 aldosterone production from zona glomerulosa cells of the adrenal cortex. *J. Physiol.*
280 **594**, 5851-5860 (2016).
- 281 34. Perez-Reyes, E., Van Deusen, A.L. & Vitko, I. Molecular pharmacology of human
282 Cav3.2 T-type Ca²⁺ channels: block by antihypertensives, antiarrhythmics, and their
283 analogs. *J. Pharmacol. Exp. Ther.* **328**, 621-7 (2009).
- 284 35. Paul, J. *et al.* Alterations in the cytoplasmic domain of CLCN2 result in altered gating
285 kinetics. *Cell. Physiol. Biochem.* **20**, 441-54 (2007).
- 286 36. Dutzler, R., Campbell, E.B., Cadene, M., Chait, B.T. & MacKinnon, R. X-ray
287 structure of a ClC chloride channel at 3.0 Å reveals the molecular basis of anion
288 selectivity. *Nature* **415**, 287-94 (2002).

289

290

291

292 **FIGURE LEGENDS**

293 **Figure 1. A *CLCN2* variant identified in a patient with early onset primary**
294 **aldosteronism.** (a) Pedigree of kindred K1011. The subject with PA is shown with a black
295 symbol and non-affected subjects are shown with white symbols. (b) Sanger sequencing
296 chromatograms showing the *CLCN2* wild-type sequence of the unaffected parents (K1011-3
297 and K1011-4) and brother (K1011-2) and the *CLCN2* variant c.71G>A (p.Gly24Asp)
298 identified in the patient with early onset primary aldosteronism (K1011-1). (c) Alignment and
299 conservation of residues encoded by *CLCN2* orthologs. The red box indicates the amino-
300 terminal 'inactivation domain' of CIC-2. Several deletions and mutations in this region of rat
301 CIC-2 led to constitutive open CIC-2 channels (uninterrupted line) or partially opened
302 channels (dashed line) ³. Residues that are conserved among more than 3 sequences are
303 highlighted in yellow. (d) Position of the disease-causing Gly24Asp mutation in the CIC-2
304 protein (schematic transmembrane topology drawing modified from ³⁶). 'Inactivation
305 domains' previously identified by structure-function analysis in the amino-terminus ³ and an
306 intracellular loop ² of CIC-2 are shown in red. Several point mutations and deletions in these
307 domains open the CIC-2 channel ^{2,3} similar to the Gly24Asp substitution described here.
308 CBS1 and CBS2, cystathionine- β -synthase domains which can affect gating of CLC channels
309 ²³.

310 **Figure 2 CIC-2 expression in mouse adrenals and electrophysiological analyses of WT**
311 **and mutant channels.** (a) CIC-2 immunoblot of brain and adrenals from *Clcn2*^{+/+} and *Clcn2*
312 ^{-/-} mice. All lanes are from the same blot, which has been cut as indicated. Similar amounts of
313 protein were loaded with actin serving as loading control. This blot is representative for three
314 independent experiments. (b) Representative whole-cell chloride current traces of mouse zona
315 glomerulosa cells from *Clcn2*^{+/+} (top) and *Clcn2*^{-/-} (bottom) adrenal slices using voltage steps
316 as indicated above. (c) Mean \pm SEM currents measured after 1.5 s from experiments in (b)

317 plotted as a function of clamp voltage. (d, e) Representative chloride current traces measured
318 by two-electrode voltage-clamp from *Xenopus* oocytes injected with either human CIC-2_{WT}
319 (d) or CIC-2_{24Asp} (e) cRNA, using the protocol shown in (d). For some measurements (below)
320 extracellular chloride was replaced with iodide. (f) Mean \pm SEM currents measured in (d,e)
321 plotted as a function of voltage. Number of cells indicated in parenthesis. (g, h) Summary of
322 Cl⁻ currents at -80 mV (I_{-80mV}) (g) and current ratios (I_{-120mV} / I_{+60mV}) as measure of
323 rectification (h) (always measured at 2s) for panels (d-f). ****p < 0.0001, Mann-Whitney
324 two-tailed test. (i, j) Effect of external pH on currents mediated by CIC-2_{WT} (i) or CIC-2_{24Asp}
325 (j) in *Xenopus* oocytes. Currents were normalized to mean currents from respective construct
326 measured after 2s at -120 mV and pH 7.4. Number of oocytes indicated in parenthesis, error
327 bars indicate SEM.

328 **Figure 3. Effect of CIC-2_{WT} and mutant CIC-2_{24Asp} channels on aldosterone production**
329 **and expression of genes and proteins involved in aldosterone biosynthesis.** (a) Western
330 blots for CIC-2 and aldosterone synthase of H295R-S2 cells stably transfected with CIC-2_{WT}
331 or mutant CIC-2_{24Asp}. These blots are representative of three independent experiments, with
332 actin serving as loading control. (b) Quantification of CIC-2 protein expression in CIC-2_{WT}
333 and CIC-2_{24Asp} H295R-S2 cells (T test p=0.10, F=3.19). (c) Quantification of aldosterone
334 synthase expression in CIC-2_{WT} or CIC-2_{24Asp} H295R-S2 cells (T test p=0.0025, F=136). (d)
335 Basal aldosterone production by H295R-S2 cells transfected with CIC-2_{WT} or mutant CIC-
336 2_{24Asp} (T test, p=0.0008, F=142). (e) Basal and stimulated aldosterone production by H295R-
337 S2 cells transfected with CIC-2_{WT} (open bars) or mutant CIC-2_{24Asp} (filled bars) (1way
338 ANOVA p<0.0001, F=23.46). (f-h) Basal and stimulated mRNA expression of (f) *CYP11B2*
339 (1way ANOVA p<0.001, F=18.39), (g) *STAR* (Kruskal-Wallis p=0.0033), and (h) *CYP21A2*
340 (1way ANOVA p<0.0001, F23.27) in H295R-S2 cells transfected with CIC-2_{WT} (open bars) or

341 mutant CIC-2_{24Asp} (filled bars). Quantification of protein expression (using actin as loading
342 control) and aldosterone production are represented as percentage of CIC-2_{WT} in basal
343 conditions and results of mRNA expression are represented as fold induction of CIC-2_{WT} in
344 basal conditions. Values of all experiments are represented as mean \pm SEM of three
345 independent experiments performed in experimental triplicates (n=9) for each condition. *
346 p<0.05; ** p<0.01; *** p<0.001; i) p<0.05 stimulated vs basal condition, ii) p<0.01
347 stimulated vs basal condition; iii) p<0.001 stimulated vs basal condition.

348 **Figure 4 Functional impact of the CIC-2_{24Asp} mutation.** (a-g) Effect on membrane
349 potential V_m and plasma membrane anion currents in H295R-S2 cells. (a) Resting membrane
350 potential of CIC-2_{WT} and CIC-2_{24Asp} stably transfected H295R-S2 cells which were used to
351 determine aldosterone secretion. Note strong mean depolarization (CIC-2_{WT}, -67 ± 2 mV
352 (n=8); CIC-2_{24Asp}, -52 ± 6 mV (n=12)), which, however, was not significant (Two-tailed
353 Mann-Whitney $p = 0.14$) owing to large variability of V_m of CIC-2_{24Asp} transfected cells that
354 were not cloned. (b) Similarly determined values of V_m for non-transfected, and transiently
355 transfected H295R-S2 cells (non-transfected, -65 ± 4 mV (n=8); CIC-2_{WT}, -69 ± 7 mV (n=4);
356 CIC-2_{24Asp}, -46 ± 4 mV (n=6); **, Two-tailed Mann-Whitney $p = 0.0095$) (c,d)
357 Corresponding plasma membrane currents measured after 1.5 s under conditions eliminating
358 cation inward currents as function of voltage (c) or as plot of individual values at
359 physiological V_m of glomerulosa cells (d) *, Two-tailed Mann-Whitney $p = 0.019$. (e-g)
360 corresponding averaged current traces with 20 mV voltage steps between 0 and -120 mV. (h-i)
361 Effect of calcium channel blockers on aldosterone production in H295R-S2 cells expressing
362 (h) CIC-2_{WT} (Kruskal Wallis $p=0.0005$) and (i) CIC-2_{24Asp} (Kruskal Wallis, $p=0.0032$). Values
363 represent mean \pm SEM of two independent experiments performed in experimental triplicates
364 (n=6) for each condition. * p<0.05; ** p<0.01.

365

366 **Figure 5. Proposed model for autonomous aldosterone secretion in adrenal zona**

367 **glomerulosa cells with the CIC-2_{24Asp} mutation.** (a) In unstimulated conditions, the ZG cell

368 membrane potential closely follows the potassium resting potential at approximately -80 mV.

369 Increasing extracellular K⁺ concentration, or inhibition of K⁺ channels by AngII through its

370 receptor (AT1R), leads to cell membrane depolarization, opening of voltage-gated Ca²⁺

371 channels, and increased intracellular calcium concentrations, the major trigger for aldosterone

372 biosynthesis. Binding of AngII to AT1R also leads to Gαq-mediated signaling and IP3-

373 mediated release of Ca²⁺ from the endoplasmic reticulum. (b) The CIC-2 p.Gly24Asn

374 mutation abolishes the voltage-dependent gating of CIC-2. The resulting pronounced increase

375 of Cl⁻ currents at resting potentials is proposed to result in cell depolarization, opening of

376 voltage gated Ca²⁺ channel, stimulation of Ca²⁺ signaling, and finally increased expression of

377 steroidogenic genes and aldosterone production.

378

379 **Table 1. Clinical and biological characteristics of patients carriers of *CLCN2* variants.**

	K1011-1	K963-1	K1044-1
Sex	F	F	F
Age at HTN dg (ys)	9	19	29
Age at primary aldosteronism dg (ys)	9	27	48
SBP at primary aldosteronism dg (mmHg)	172	139	173
DBP at primary aldosteronism dg (mmHg)	100	90	114
Lowest plasma K⁺ (mmol/L)	1.8	2.9	2.5
Urinary aldosterone (nmol/24h)	ND	60	ND
Plasma aldosterone (pmol/L)^a	2406	927	1061
Plasma renin (mU/L)^a	0.9	1.9	<1
ARR (pmol/mU)^b	481.2	185.4	212.2
Adrenal abnormalities on imaging	No	No	No
Lateralization at AVS	ND	No	No

380 dg, diagnosis; m, months; y, years ; HTN, hypertension; SBP, systolic blood pressure; DBP, diastolic
381 blood pressure; K, potassium; ARR, aldosterone to renin ratio; Hormonal data are at diagnosis of
382 primary aldosteronism. ND, not determined. For comparison within this table, plasma aldosterone
383 levels for patient K1011-1 have been converted to pmol/L and plasma renin activity to plasma renin
384 concentration. ^bfor ARR calculation, renin values <5 have been transformed to 5. Conversion factor
385 used for plasma aldosterone: 1 ng/l = 2.77 pmol/L; conversion factor used for plasma renin: 1 ng/ml/h
386 = 8.2 mU/L.

387

388 **Online Methods**

389 ***Patients***

390 Patients with primary aldosteronism were recruited within the COMETE (Cortico- et
391 MEdullo-surrénale, les Tumeurs Endocrines) network (COMETE-HEGP protocol,
392 authorization CPP 2012-A00508-35) or in the context of genetic screening for familial
393 hyperaldosteronism at the Genetics department of the HEGP. Methods for screening and
394 subtype identification of primary aldosteronism were performed according to the Endocrine
395 Society guidelines⁸. In patients diagnosed with primary aldosteronism, a thin slice CT scan or
396 MRI of the adrenal and/or an adrenal venous sampling (AVS) were performed to differentiate
397 between unilateral and bilateral aldosterone hypersecretion. All patients gave written
398 informed consent for genetic and clinical investigation. Procedures were in accordance with
399 institutional guidelines.

400

401 ***DNA isolation***

402 DNA from peripheral blood leukocytes was extracted using QIAamp DNA midi kit (Qiagen,
403 Courtaboeuf Cedex, France) or salt-extraction.

404

405 ***Whole exome sequencing and variant detection***

406 Exomes were enriched in solution and indexed with SureSelect XT Human All Exon 50 Mb
407 kits (Agilent). Sequencing was performed as 100 bp paired-end runs on HiSeq2000 systems
408 (Illumina). Pools of 12 indexed libraries were sequenced on four lanes. Image analysis and
409 base calling was performed using Illumina Real Time Analysis. CASAVA 1.8 was used for
410 demultiplexing. BWA (v 0.5.9) with standard parameters was used for read alignment against
411 the human genome assembly hg19 (GRCh37). We performed single-nucleotide variant and
412 small insertion and deletion (indel) calling specifically for the regions targeted by the exome

413 enrichment kit, using SAMtools (v 0.1.18). Subsequently the variant quality was determined
414 using the SAMtools varFilter script. We used default parameters, with the exception of the
415 maximum read depth (-D) and the minimum P-value for base quality bias (-2), which we set
416 to 9999 and 1e-400, respectively. Additionally, we applied a custom script to mark all
417 variants with adjacent bases of low median base quality. All variants were then annotated
418 using custom Perl scripts. Software is available on request (<https://ihg4.helmholtz->
419 [muenchen.de/cgi-bin/mysql/snv-vcf/login.pl](https://ihg4.helmholtz-muenchen.de/cgi-bin/mysql/snv-vcf/login.pl)). Annotation included information about known
420 transcripts (UCSC Known Genes and RefSeq genes), known variants (dbSNP v 135), type of
421 mutation, and - if applicable – amino acid change in the corresponding protein. The annotated
422 variants were then inserted into our in-house database. To reduce false positives we filtered
423 out variants that were already present in our database, had variant quality less than 40, or
424 failed one of the filters from the filter scripts. We then manually investigated the raw read
425 data of the remaining variants using the Integrative Genomics Viewer (IGV).
426

427 ***Sanger sequencing***

428 *CLCN2* DNA was amplified using the intron-spanning primers described in supplementary
429 table S2. PCR were performed on 100 ng of DNA in a final volume of 25 μ l containing 0.75
430 mM MgCl₂, 400 nM of each primer, 200 μ M deoxynucleotide triphosphate, and 1.25 U Taq
431 DNA Polymerase (Sigma). Cycling conditions for *CLCN2* were as previously described³⁷
432 with an annealing temperature of 60°C. Direct sequencing of PCR products was performed
433 using the ABI Prism Big Dye Terminator® v3.1 Cycle Sequencing Kit (Applied Biosystems,
434 Foster City, CA) on an ABI Prism 3700 DNA Analyzer (Applied Biosystems).

435

436 ***Site directed mutagenesis***

437 The CIC-2_{24Asp} construct was generated by site-directed mutagenesis using the QuikChange II
438 XL site-directed mutagenesis kit (Agilent). The mutation was introduced into the human CIC-
439 2 cDNA fragment inserted into the pFROG expression vector³⁸ and their presence confirmed
440 by Sanger sequencing.

441

442 ***Western blot***

443 The membrane fractions of tissue homogenate from brain and adrenal gland of adult *Clcn2*^{+/+}
444 and *Clcn2*^{-/-} mice were isolated and lysed in 50mM Tris pH 6.8, 140mM NaCl, 0.5mM
445 EDTA and 2% SDS with protease inhibitors (4 mM Pefabloc and Complete® EDTA-free
446 protease inhibitor cocktail, Roche). Equal amounts of protein were separated by SDS-PAGE
447 (10 % polyacrylamide) and blotted onto nitrocellulose. Rabbit polyclonal antibodies against a
448 modified carboxy-terminal CIC-2 peptide have been described previously²⁶. Blots were
449 reprobed with mouse anti- β -actin (Clone AC-74, Sigma A2228, 1:1000) as a loading control.
450 H295R-S2 cells were lysed using RIPA buffer (Bio Basic Canada Inc.) with protease and
451 phosphatase inhibitors mini tablets, EDTA free (Thermo Scientific). Proteins were solubilized

452 for 30 min at 4°C, under end-over-end rotation, and then centrifuged at 13000 rpm for 15 min
453 at 4°C. Equal amounts of proteins were submitted to 10% SDS-PAGE and transferred onto
454 nitrocellulose membrane. Membranes were blotted with rabbit anti-CIC-2 antibody (1:500),
455 mouse anti-aldosterone synthase antibody (1:500, clone CYP11B2-41-13, kindly provided by
456 Dr C Gomez Sanchez³⁹) and mouse anti-β-actin (A2228, 1:10000, Sigma).

457

458

459 *Electrophysiological recordings*

460 Patch clamp analysis were performed in adrenal sections from wild type and *Cln2*^{-/-} mice²⁴,
461 similarly to previously described⁴⁰. Bicarbonate based buffers were used which were
462 continuously bubbled with 95% O₂ and 5% CO₂. Briefly, adrenal glands were removed and
463 placed into cold low-Ca²⁺ solution composed of (in mM): 140 NaCl, 2 KCl, 26 NaHCO₃, 10
464 glucose, 5 MgCl₂, 0.1 CaCl₂, pH 7.4. The adrenals, after removal of surrounding fat tissue,
465 were embedded in 3% low-melting agarose, sectioned at 70 μm (Leica VT1200S), and
466 incubated at room temperature in solution containing: 140 NaCl, 2 KCl, 26 NaHCO₃, 10
467 glucose, 2 MgCl₂, 2 CaCl₂, and adjusted to pH 7.4. After at least 1 hour, slices were then
468 transferred to a recording chamber and imaged with a 60x objective and DIC optics (Olympus
469 BX51WI). Cells of the zona glomerulosa were identified by their rosette organization.
470 Electrical signals were acquired at room temperature using a microelectrode amplifier
471 (Multiclamp 700B) and software (Clampex 10.3, Molecular Devices, USA). As expected,
472 cells when patched with a K⁺-based solution displayed spontaneous spiking which could be
473 stimulated with angiotensin II. For measuring chloride currents, patch pipettes were filled
474 with solution containing: 117.5 CsMeSO₃, 17.5 CsCl, 4 NaCl, 10 Hepes, 1 EGTA, 1 MgCl₂,
475 adjusted to pH 7.3 while the bath solution contained: 117 NMDG-Cl, 23 NMDG-HCO₃, 5
476 CsCl, 1.3 MgCl₂, 9 glucose, 2 CaCl₂, adjusted to pH 7.3. Voltage steps from +40 to -120 mV

477 from a holding potential of -10 mV were used, with a final 1 s step at $+40$ mV. Signals were
478 digitized at 10 kHz, filtered at 2 kHz and stored off-line for analysis with Clampfit software
479 10.4.

480 For two electrode voltage clamp in *Xenopus laevis* oocytes, human wildtype and Gly24Asp
481 CIC-2 cRNAs were prepared from pFROG vectors (Ambion mMACHINE T7
482 kit) and injected into *X. laevis* oocytes, 13.8 ng and 9.2 ng per cell, respectively. Following
483 two days of expression at 17°C , two electrode voltage clamp was performed at room
484 temperature using a TurboTEC amplifier (npi electronic GmbH, Tamm, Germany) and
485 pClamp Software (Molecular Devices) to elicit CIC-2 currents (2s steps from $+60$ mV to -
486 120 mV with a final 1s step at $+40$ mV) in ND109 solution containing (in mM): 109 NaCl, 2
487 KCl, 1 MgCl₂, 1.8 CaCl₂, 2 HEPES and adjusted to pH 7.4. To test for the typical Cl⁻>I⁻
488 selectivity of CLC channels, currents were sequentially measured in solutions containing 109
489 mM Cl⁻ or 109 mM I⁻. To determine the pH sensitivity of currents, ND109 was buffered with
490 5 mM MES for pH 6.5 and with 5 mM Tris for pH 8.5. Off-line analysis was performed with
491 Clampfit software 10.4. Statistical significance was assessed using the Mann–Whitney test
492 (Prism, GraphPad Software, USA).

493 For patch clamp of transiently transfected H295R-S2 cells, cells were seeded at 30%
494 confluency onto poly-L-lysine (Sigma) coated glass coverslips. Once adhered they were
495 transfected (X-fect) with bicistronic plasmids encoding emGFP (for identification of
496 transfected cells) and, after an IRES sequence, CIC-2_{WT} or CIC-2_{G24D}. Cells were
497 measured 12-24 hours later. Both transiently and stably transfected cells were measured
498 using a Multiclamp 700B (Axon Instruments) amplifier Gramicidin-perforated patch clamp
499 was performed to retain the intracellular chloride concentration. The tips of patch pipettes
500 were first filled with gramicidin-free internal pipette solution (in mM): 100 KMeSO₃, 30 KCl,
501 4 NaCl, 10 Hepes, 1 MgCl₂, 1 EGTA, 3 MgATP (pH 7.3, 280 mOsm/L) and then back-filled

502 with the same solution containing 25µg/mL gramicidin. GFP expressing cells were selected
503 for analysis. Approximately 20 minutes following tight giga-seal formation, stable membrane
504 potential measurements (I=0 configuration) could be acquired with access resistances of <100
505 MΩ in bath solution containing 140 NaCl, 5 KCl, 10 Hepes, 1.8 MgCl₂, 1.8 CaCl₂ (pH 7.4,
506 300 mOsm/L). When adequate access resistance was attained (<35 MΩ), a Na⁺- and K⁺-free
507 bath solution containing 140 CsCl, 10 Hepes, 1.8 MgCl₂, 1.8 CaCl₂, 20 sucrose (pH 7.3, 300
508 mOsm/L) was perfused to measure anion membrane currents in the voltage clamp
509 configuration (1s steps from +60 mV to -120 mV from a holding clamp of -10 mV).
510 Measurements were performed at room temperature (22-24°C). Data are presented as mean
511 ± SEM.

512

513 *Functional studies in H295R-S2 cells*

514 The human adrenocortical carcinoma cell line H295R strain 2 (H295R-S2), kindly
515 provided by W. E. Rainey⁴¹ was cultured in DMEM/Eagle's F12 medium (GIBCO, Life
516 technologies, Carlsbad, CA) supplemented with 2% Ultrosor G (PALL life sciences, France),
517 1% insulin/transferrin/selenium Premix (GIBCO, Life technologies, Carlsbad, CA), 10mM
518 HEPES (GIBCO, Life technologies, Carlsbad, CA), 1% penicillin, and streptomycin (GIBCO,
519 Life technologies, Carlsbad, CA) and maintained in a 37°C humidified atmosphere (5%
520 CO₂).

521 For overexpression experiments, H295R-S2 cells were seeded into tissue culture dishes 100 in
522 groups of 5.000.000 cells per dish, and maintained in the conditions described. After 24h,
523 cells were resuspended in 100 µl Nucleofector R solution (AMAXA kit, Lonza) and
524 transfected with 3 µg of the ClC-2_{WT} or ClC-2_{24Asp} pFROG construct or a GFP construct,
525 using the electroporation program P-20. To select only stably transfected cells, 48h post
526 transfection cells were changed to medium containing 500 µg/mL G418-Genetycin (Gibco)

527 and used after all GFP transfected cells were dead. G418 selection was kept during all
528 functional studies. For aldosterone measurements and RNA extraction, cells were serum
529 deprived in DMEM/F12 containing 0.1% Ultrosor G for 24h and then incubated for another
530 24h with fresh medium containing 0.1% Ultrosor G with no secretagogue or vehicle (basal),
531 or secretagogues AngII (10nM) or K^+ (12mM), or calcium channel blockers Nifedipine (L-
532 Type calcium channel blocker, 10 μ M, Sigma) or Mibefradil (T-type calcium channel
533 blocker, 10 μ M, Sigma). At the end of the incubation time, supernatant and cells from each
534 well were harvested for aldosterone measurement and RNA extraction. Three experiments
535 using aldosterone secretagogues (n=9) and two experiments using calcium channel blockers
536 (n=6) were independently conducted in triplicate.

537 Human CIC2-targeting (TRCN0000427876) and non-mammalian control (SHC002V)
538 MISSION shRNA lentiviral transduction particles were obtained from Sigma-Aldrich. The
539 shRNA sequences were inserted into TRC2 pLKO-puro plasmid backbone. For the lentiviral
540 infections, manufacturer's protocol was followed with slight modifications. 1×10^4 H295R-S2
541 cells were seeded in a 96-well plate. After 24 hours, medium was changed and supplemented
542 with 2 μ g/ml polybrene (Sigma). Lentiviral particles were then added at a multiplicity of
543 infection of 10 and medium changed after overnight incubation. For selection, 2 μ g/ml
544 puromycin (Gibco) was added to the medium. After two passages cells were characterized in
545 terms of mRNA expression and aldosterone production after incubation with or without
546 secretagogue as mentioned above.

547

548 ***RNA extraction and RT-qPCR***

549 Total RNA was extracted in Trizol reagent (Ambion Life technologies, Carlsbad CA)
550 according to the manufacturer's recommendations. After deoxyribonuclease I treatment (Life
551 Technologies, Carlsbad, CA), 500 ng of total RNA were retrotranscribed (iScript reverse

552 transcriptase, Biorad, Hercules, CA). Primers used for qPCR are described in supplementary
553 table 3. The quantitative PCR was performed using SYBRgreen (Sso advanced universal
554 SyBr Green supermix, Biorad, Hercules, CA) on a C1000 touch thermal cycler of Biorad
555 (CFX96 Real Time System), according to the manufacturer's instructions. Controls without
556 template were included to verify that fluorescence was not overestimated from primer dimer
557 formation or PCR contaminations. RT-qPCR products were analyzed in a post amplification
558 fusion curve to ensure that a single amplicon was obtained. Normalization for RNA quantity,
559 and reverse transcriptase efficiency was performed against three reference genes (geometric
560 mean of the expression of Ribosomal *18S* RNA, *HPRT*, and *GAPDH*), in accordance with the
561 MIQE guidelines ⁴². Quantification was performed using the standard curve method. Standard
562 curves were generated using serial dilutions from a cDNA pool of all samples of each
563 experiment, yielding a correlation coefficient of at least 0.98 in all experiments.

564

565 ***Aldosterone and protein assays***

566 Aldosterone levels were measured in cell culture supernatants by ELISA. Aldosterone
567 antibody and aldosterone-3-CMO-biotin were kindly provided by Dr Gomez-Sanchez ⁴³.
568 Aldosterone concentrations were normalized to cell protein concentrations (determined using
569 Bradford protein assay).

570

571 ***Statistical analyses***

572 Quantitative variables are reported as means \pm standard error of the mean (SEM) when
573 Gaussian distribution or medians and interquartile range when no Gaussian distribution.
574 Pairwise comparisons were done with unpaired t-test or Mann-Whitney test respectively;
575 multiple comparisons were done with the ANOVA test followed by a test for pairwise
576 comparison of subgroups according to Bonferroni when Gaussian distribution, or Kruskal-

577 Wallis followed by Dunn's test when no Gaussian distribution. Comparisons between two
578 groups were performed with two-tailed T test or two-tailed Mann-Whitney test. A p value <
579 0.05 was considered significant. For functional experiments, all results were expressed as
580 mean \pm SEM of three separate experiments performed in triplicate for CIC-2 overexpression
581 studies with secretagogues, two separate experiments performed in triplicate for CIC-2
582 expression studies with calcium channel blockers, and two to four separate experiments
583 performed in triplicate for CIC-2 knockdown studies. Analyses were performed using Prism5
584 (GraphPad software Inc, San Diego, CA).

585

586 **Data availability.**

587 The data that support the findings of this study are available from the authors on reasonable
588 request, see author contributions for specific data sets. Disease-causing variants have been
589 submitted to ClinVar. Exome data are available on request within a scientific cooperation.

590 **Online Methods References**

- 591 37. Hubert, E.L. *et al.* Mineralocorticoid receptor mutations and a severe recessive
592 pseudohypoaldosteronism type 1. *J. Am. Soc. Nephrol.* **22**, 1997-2003 (2011).
- 593 38. Gunther, W., Luchow, A., Cluzeaud, F., Vandewalle, A. & Jentsch, T.J. CIC-5, the
594 chloride channel mutated in Dent's disease, colocalizes with the proton pump in
595 endocytotically active kidney cells. *Proc. Natl. Acad. Sci. U S A* **95**, 8075-80 (1998).
- 596 39. Gomez-Sanchez, C.E. *et al.* Development of monoclonal antibodies against human
597 CYP11B1 and CYP11B2. *Mol. Cell. Endocrinol.* **383**, 111-7 (2014).
- 598 40. Hu, C., Rusin, C.G., Tan, Z., Guagliardo, N.A. & Barrett, P.Q. Zona glomerulosa cells
599 of the mouse adrenal cortex are intrinsic electrical oscillators. *J. Clin. Invest.* **122**,
600 2046-53 (2012).

- 601 41. Wang, T. *et al.* Comparison of aldosterone production among human adrenocortical
602 cell lines. *Horm. Metab. Res.* **44**, 245-50 (2012).
- 603 42. Bustin, S.A. *et al.* The MIQE guidelines: minimum information for publication of
604 quantitative real-time PCR experiments. *Clin. Chem.* **55**, 611-22 (2009).
- 605 43. Gomez-Sanchez, C.E. *et al.* The production of monoclonal antibodies against
606 aldosterone. *Steroids* **49**, 581-7 (1987).
- 607

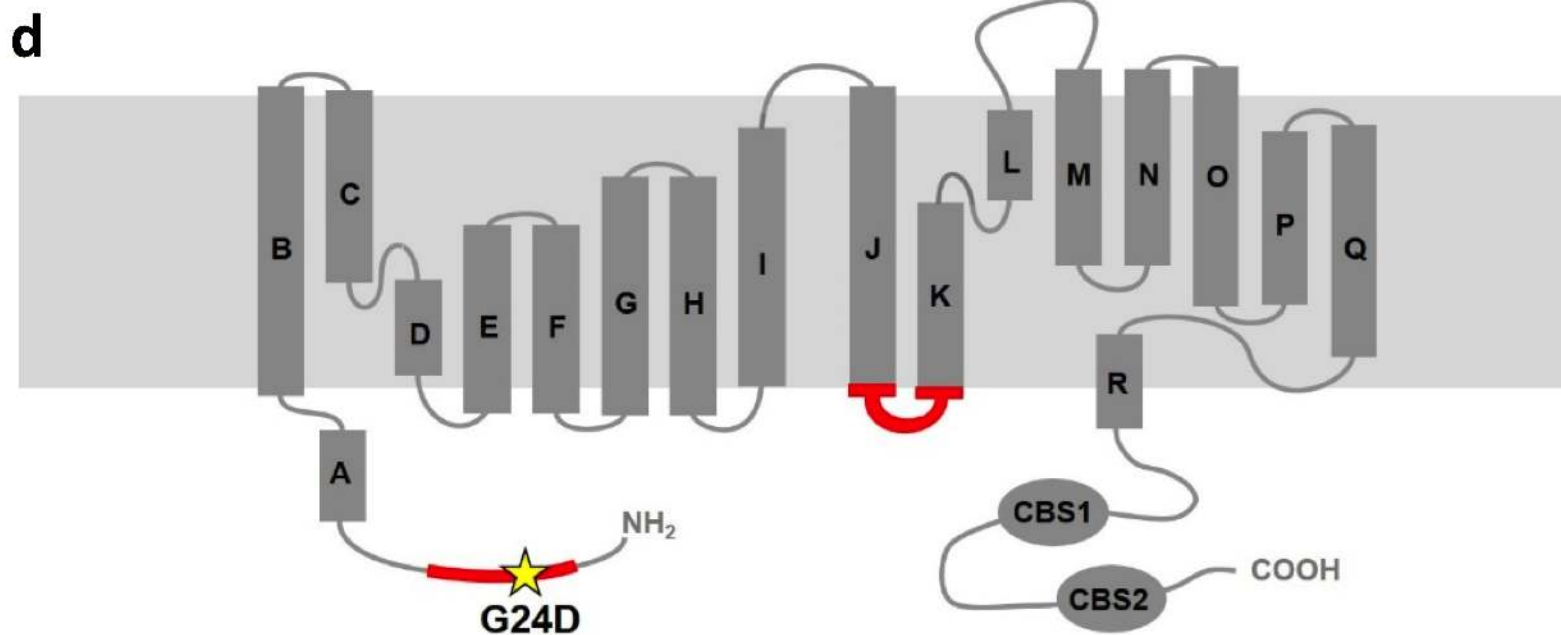
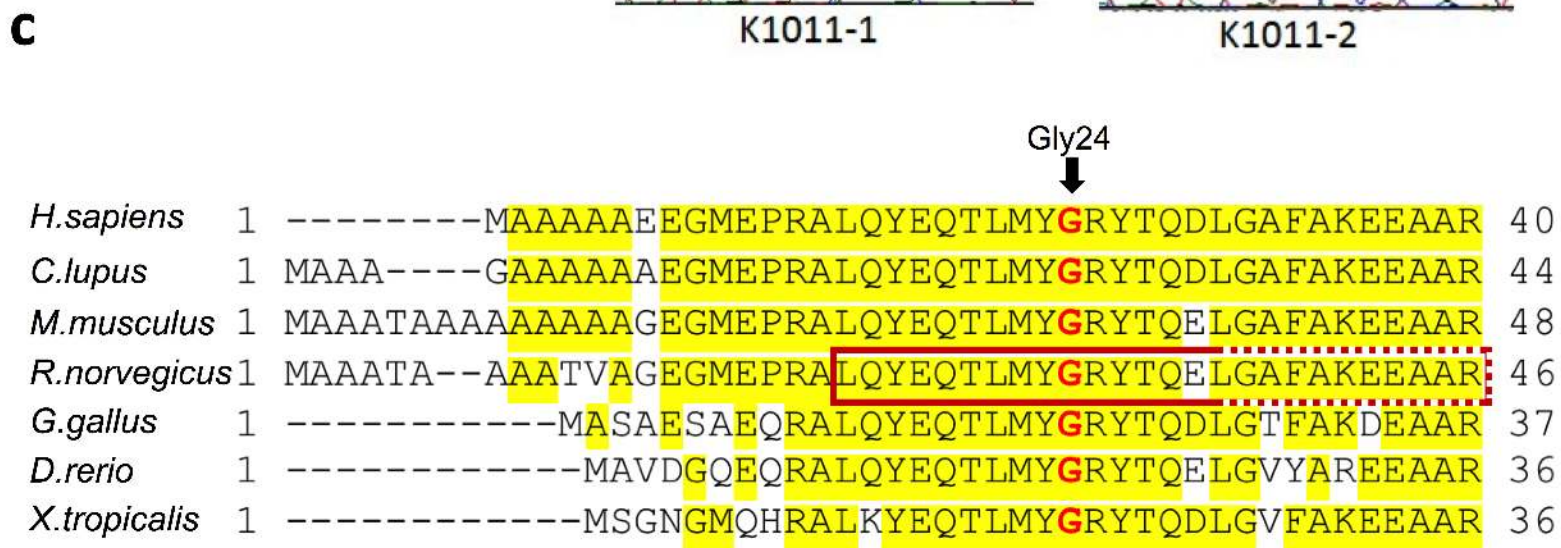
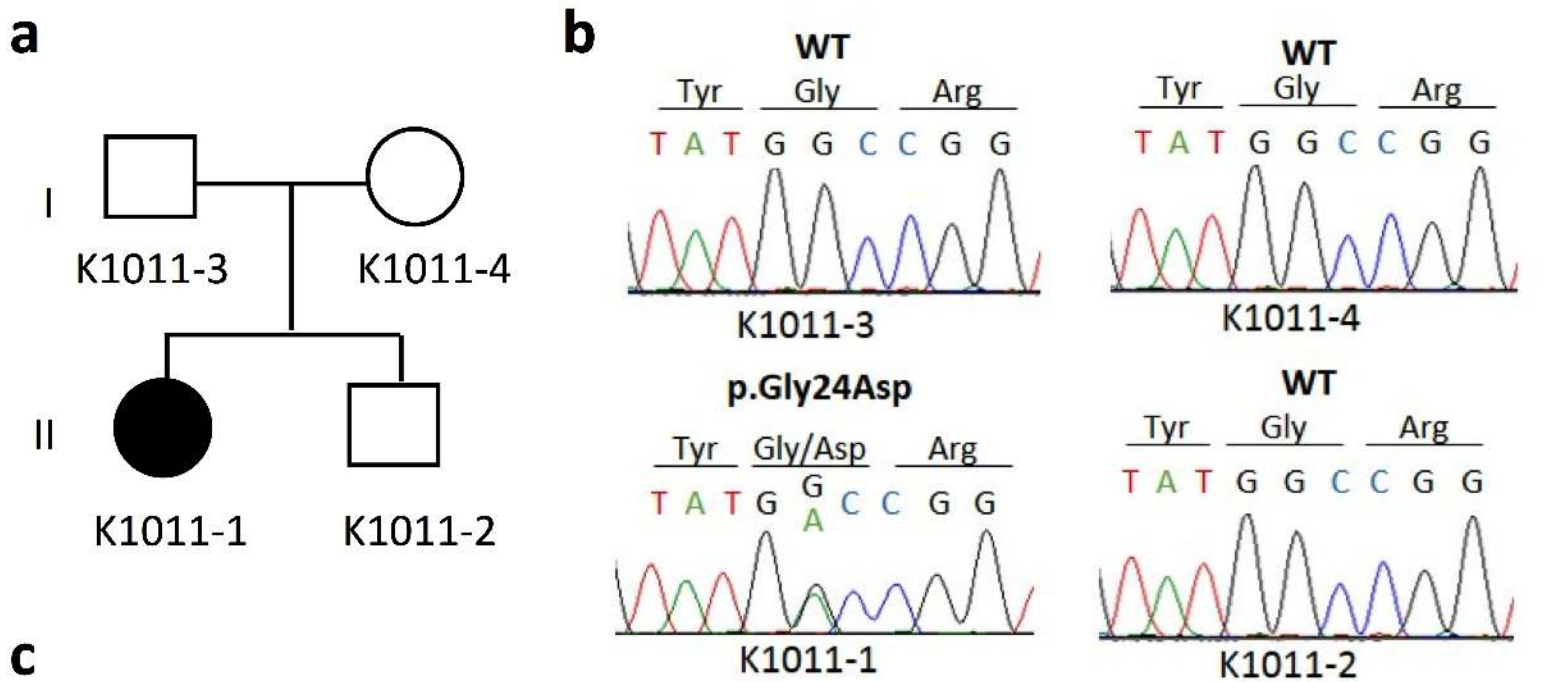


Figure 1

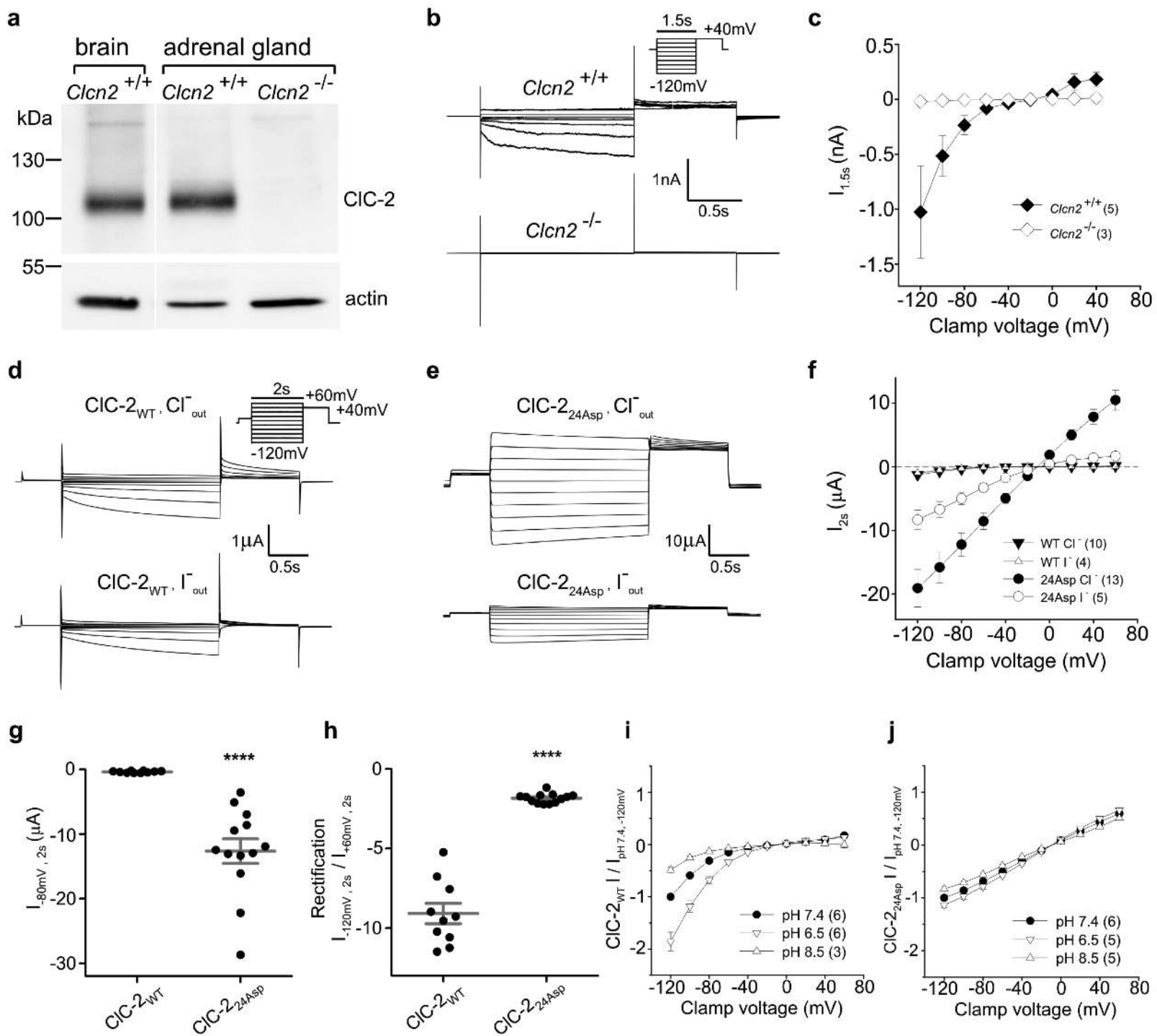


Figure 2

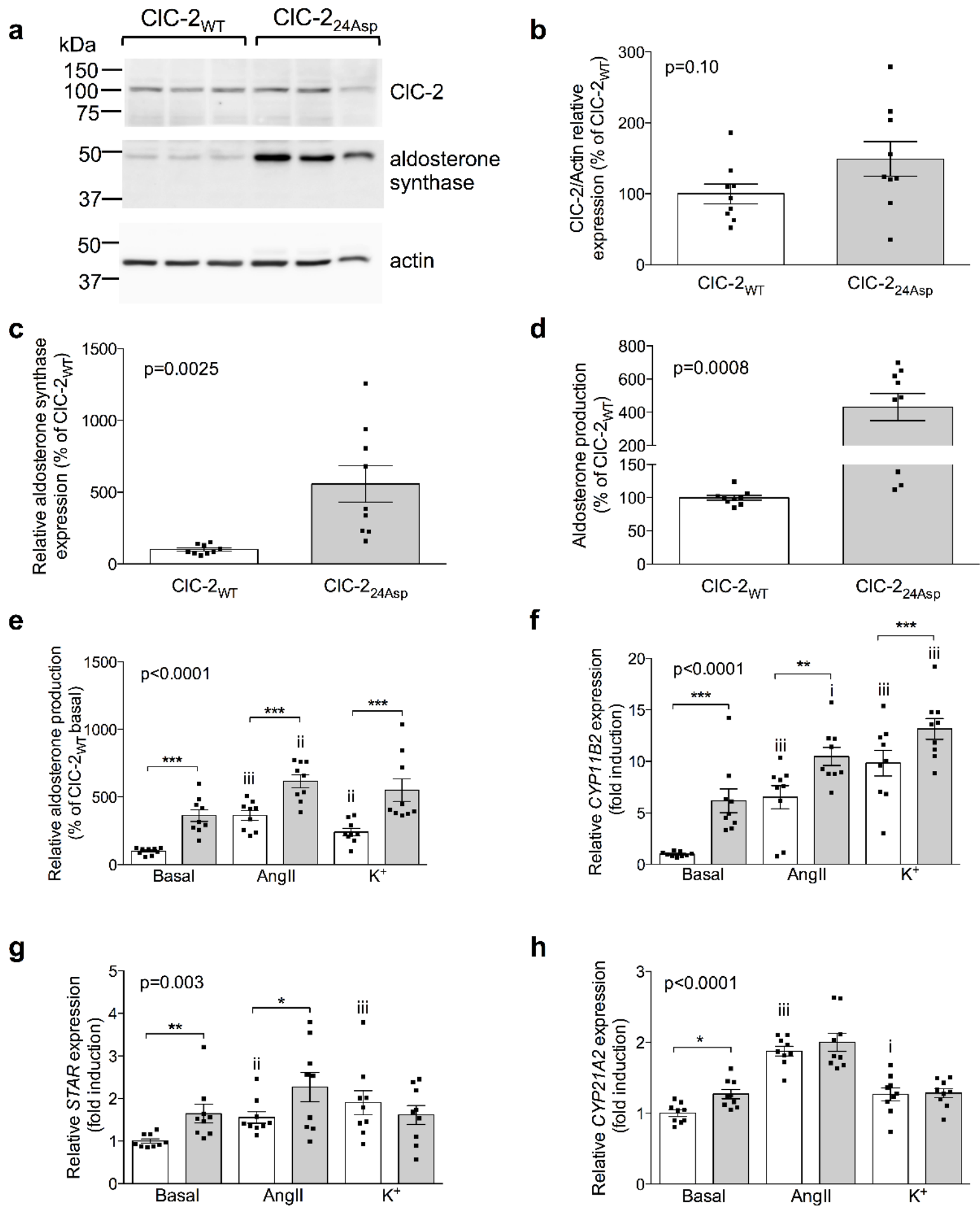


Figure 3

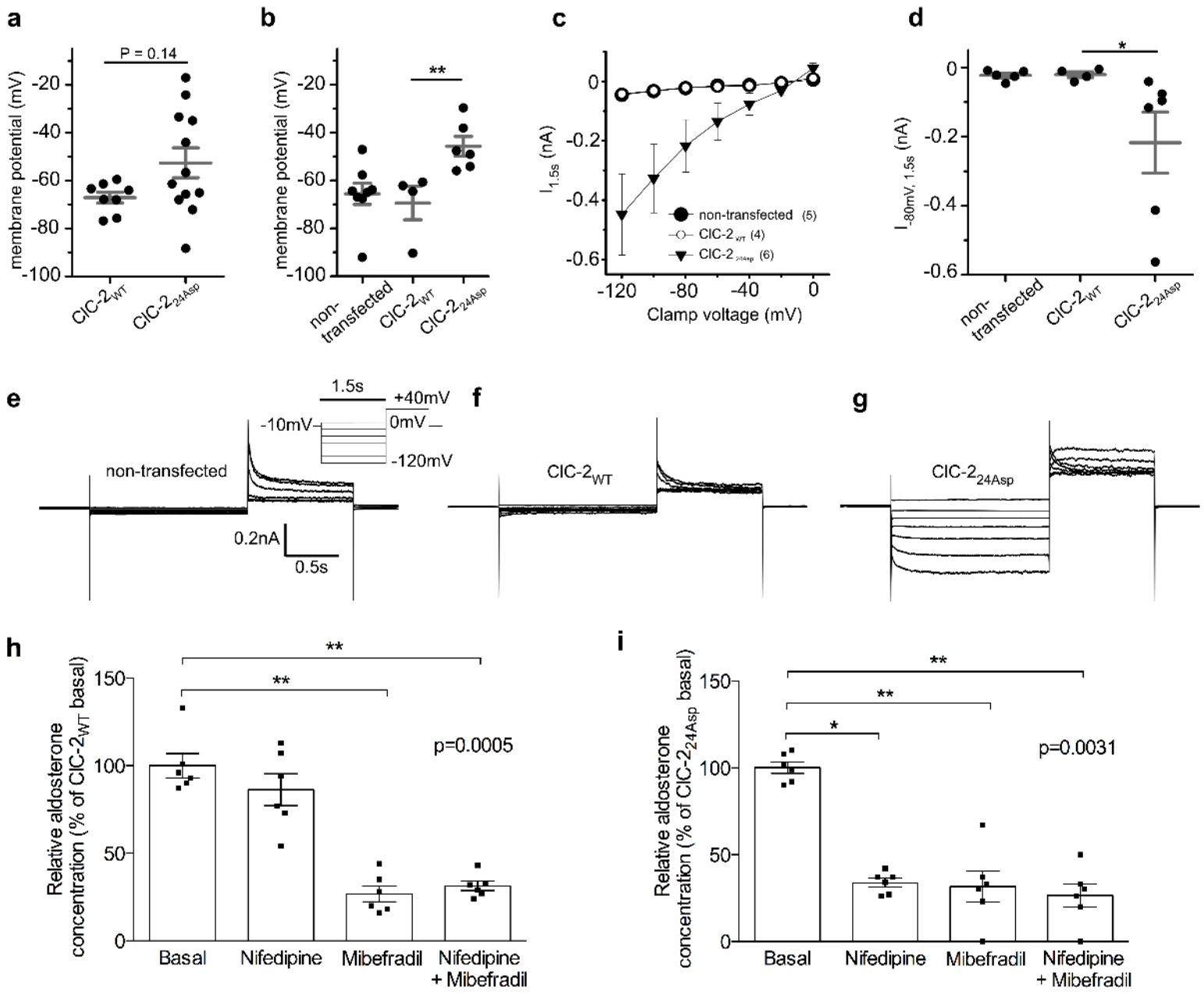


Figure 4

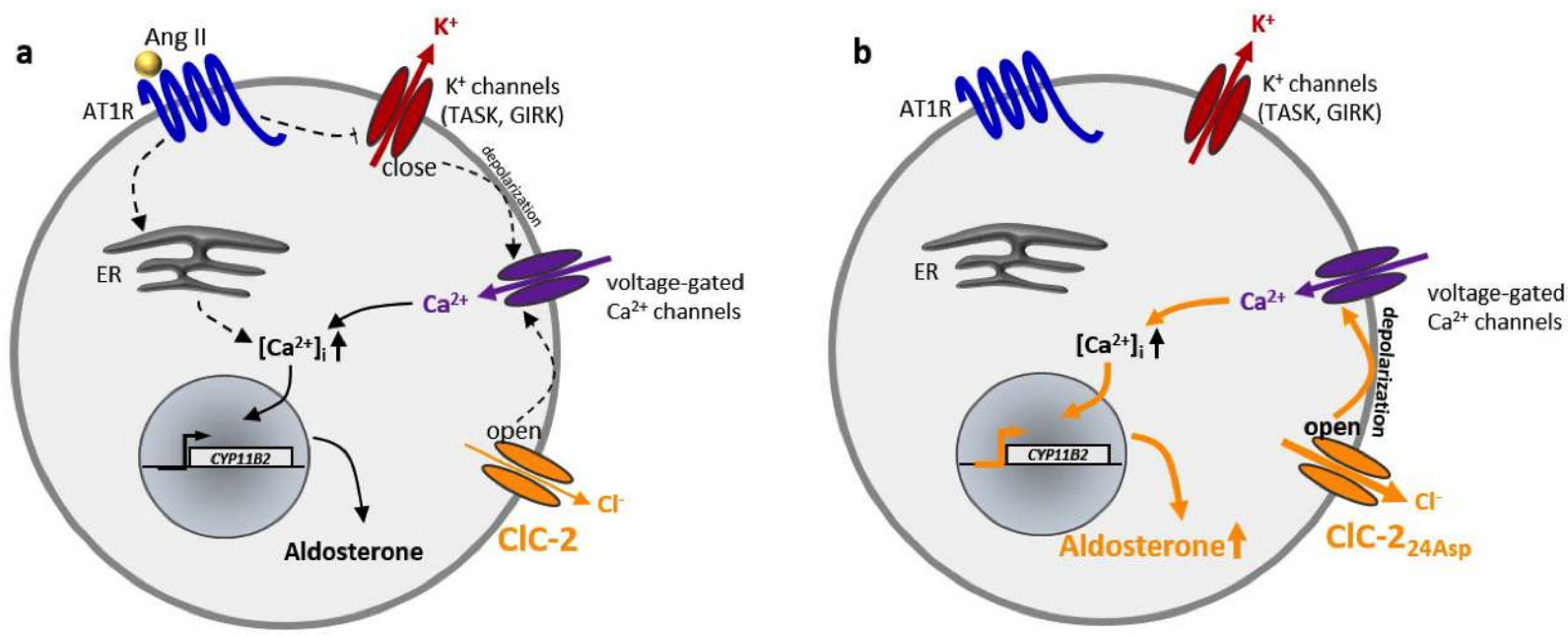


Figure 5